A unified solution for self-equilibrium and super-stability of rhombic truncated regular polyhedral tensegrities

Li-Yuan Zhang [a], Yue Li [b], Yan-Ping Cao [a], Xi-Qiao Feng [a,*]

[a] CNMM & AML, Department of Engineering Mechanics, Tsinghua University, Beijing 100084, China
[b] Institute of Nuclear and New Energy Technology, Tsinghua University, Beijing 100084, China

A B S T R A C T

As a novel class of lightweight and reticulated structures, tensegrities have found a diversity of technologically significant applications. In this paper, we theoretically investigate the self-equilibrium and super-stability of rhombic truncated regular polyhedral (TRP) tensegrities. First, the analytical solutions are derived individually for rhombic truncated tetrahedral, cubic, octahedral, dodecahedral, and icosahedral tensegrities. Based on these solutions, we establish a unified analytical expression for rhombic TRP tensegrities. Then the necessary and sufficient condition that ensures the existence of a self-equilibrated and super-stable state is provided. The obtained solutions are helpful not only for the design of self-equilibrated and super-stable tensegrities but also for their applications in biomechanics, civil and aerospace engineering.

© 2012 Elsevier Ltd. All rights reserved.

1. Introduction

Tensegrity, a structure based on the complementary equilibrium of axial tension and compression, is perceived as a potential solution to many practical problems (Skelton and de Oliveira, 2009). In nature, tensegrity can be considered as a generic principle in organisms ranging from molecules (Luo et al., 2008; Morrison et al., 2011), cells (Holst et al., 2010; Stamenovic and Ingber, 2009) to tissues (Maina, 2007). In industry, tensegrity has a variety of important applications in, for instance, the development of advanced materials (Fraternali et al., 2012), novel civil architectures (Rhode-Barbarigos et al., 2010; Yuan et al., 2007), smart structures and systems (Ali and Smith, 2010; Moored et al., 2011), and deployable devices for aerospace technology (Sultan, 2009).

In the design of a tensegrity structure, two key steps, among others, are self-equilibrium and stability analyses to determine the conditions under which the structure will be self-equilibrated and stable, respectively (Zhang et al., 2012). The existing self-equilibrium analysis methods can be generally classified into two categories, analytical and numerical. Analytical approaches can be used only for simple tensegrities with high symmetry (e.g. Murakami and Nishimura, 2001; Zhang and Ohsaki, 2012), while numerical methods are often invoked for relatively complicated tensegrities (e.g. Estrada et al., 2006; Li et al., 2010b; Pagitz and Tur, 2009). The criterion of super-stability provides a sufficient condition for the stability of a tensegrity structure consisting of

conventional material elements with always positive axial stiffness (Guest, 2011; Schenk et al., 2007; Zhang and Ohsaki, 2007). In the present paper, only the static stability is considered, excluding the instability problems caused by non-conservative disturbances. A tensegrity structure is said to be super-stable if it is stable for any level of force densities satisfying the self-equilibrium conditions without causing element material failure (Connelly, 1999; Juan and Tur, 2008). For the self-equilibrated and super-stable tensegrities, increasing the level of force densities normally tend to stiffen and stabilize them (Connelly and Back, 1998). This property is important for the constructions and applications of tensegrities.

In practice, a tensegrity structure is generally modelled as a set of weightless axial compressive elements (called 'bars' or 'struts') and tensile elements ('strings' or 'cables') connected by frictionless spherical joints (Juan and Tur, 2008). One can construct tensegrities by assembling a certain number of elementary cells according to certain design rules (Feng et al., 2010; Li et al., 2010a). Based on the local configuration of each constituent elementary cell, Pugh (1976) defined two major classes of tensegrities, called Z-based (or zig-zag) structures and rhombic (or diamond) structures, respectively (Feng et al., 2010). In the past decade, the self-equilibrium and stability of some Z-based truncated regular polyhedral (TRP) tensegrities have been investigated by using either analytical or numerical methods (e.g. Koohestani, 2012; Li et al., 2010b; Murakami and Nishimura, 2001, 2003; Pandia Raj and Guest, 2006; Zhang and Ohsaki, 2012). Recently Zhang et al. (2012) derived a unified analytical solution for the self-equilibrium and super-stability of all Z-based TRP tensegrities. In recognition to

---

* Corresponding author. Tel.: +86 10 62772934; fax: +86 10 62781824.
  E-mail address: fengxq@tsinghua.edu.cn (X.-Q. Feng).

their important applications in, for instance, cytoskeleton (Ingber, 2010; Pirentis and Lazopoulos, 2010), the self-equilibrium and sta-bility of rhombic expandable octahedron tensegrities have been studied by some researchers (e.g. Lazopoulos, 2005; Xu and Luo, 2011; Zhang and Ohsaki, 2006). However, the properties of self-equilibrium and super-stability of rhombic TPR tensegrities, an important class of tensegrity structures of extensive interest, are still unclear.

Therefore, the present study aims at exploring the self-equilibrium and stability properties of rhombic TRP tensegrities. The paper is organized as follows. In Section 2, the concepts of Z-based TRP tensegrities and rhombic TRP tensegrities are briefly reviewed. Section 3 gives the theoretical basis for the self-equilibrium and super-stability of tensegrities. Sections 4 and 5 analyze, respectively, the self-equilibrium and super-stability of rhombic truncated tetrahedral, cubic/octahedral, and dodecahe-dral/icosahedral tensegrities. Section 6 establishes a unified solution for the necessary and sufficient condition that ensures the existence of self-equilibrated and super-stable states for all types of rhombic TRP tensegrities.

2. TRP tensegrities

2.1. Z-based TRP tensegrities

To facilitate subsequent analysis, we refer to the following def-inition of polyhedra (Coxeter, 1973):

Definition 1. A regular polyhedron can be uniquely identified by the Schläfli symbol $\{n, m\}$, where n is the number of edges in each face and m is the number of faces around each vertex.

In total, there are five types of convex regular polyhedra (Cromwell, 1997), including tetrahedron identified by $\{3, 3\}$, cube $\{4, 3\}$, octahedron $\{3, 4\}$, dodecahedron $\{5, 3\}$, and icosahedron $\{3, 5\}$, as shown in Fig. 1(a). By cutting off each vertex of these regular polyhedra, one can obtain the five types of truncated regular polyhedra, as shown in Fig. 1(b).

In a Z-based TRP tensegrity structure, each string corresponds to an edge of the truncated regular polyhedron and the bars con-nect the vertexes by following the rule of Z-shaped elementary cells (Li et al., 2010a). For illustration, we take the construction of a Z-based truncated tetrahedral tensegrity as an example. In the first step, one truncates a tetrahedron by cutting all its original vertices and creating a new polygonal facet around each vertex. Fig. 2(a) shows the vertices and edges of the truncated tetrahedron. Then, the strings and bars are added following the procedure pro-posed by Li et al. (2010a). Fig. 2(b) illustrates the nodes, strings, and bars of the tensegrity, where a Z-shaped cell, consisting of the nodes 1–4, is highlighted. Fig. 1(c) gives the five types of Z-based TRP tensegrities corresponding to the polyhedra in Fig. 1(a) and the truncated polyhedra in Fig. 1(b).

2.2. Rhombic TRP tensegrities

A rhombic cell in self-equilibrated tensegrities has the similar load-bearing feature as a Z-shaped cell (Feng et al., 2010), as shown in Fig. 3. In both elements, the external forces should be applied in a certain range of direction such that the bar is under compression and the strings are under tension. In other words, the nodes 1 and 3 tend to approach each other while the nodes 2 and 4 tend to sep-arate. Therefore, a rhombic tensegrity structure can be simply con-structed from a Z-based tensegrity structure by simply replacing all its Z-shaped cells with rhombic cells. For example, based on the Z-based truncated tetrahedral tensegrity in Fig. 2(b), a rhombic truncated tetrahedral tensegrity can be readily built, as shown in
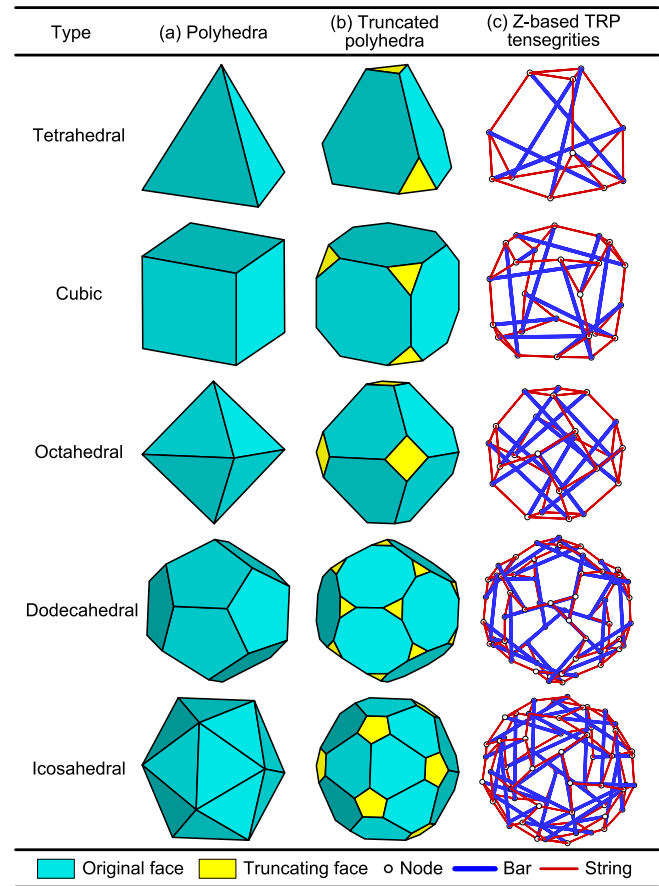

Type	(a) Polyhedra	(b) Truncated polyhedra	(c) Z-based TRP tensegrities
Tetrahedral			
Cubic			
Octahedral			
Dodecahedral			
Icosahedral			

Original face   Truncating face   ○ Node   ▬ Bar   — String

Fig. 1. Polyhedra and Z-based tensegrities: (a) regular polyhedra, (b) truncated regular polyhedra, and (c) Z-based TRP tensegrities.

Fig. 2(c). The Z-shaped cell highlighted in Fig. 2(b) has been re-placed by the rhombic cell highlighted in Fig. 2(c).

However, it is emphasized that corresponding to the five types of Z-based TRP tensegrities, there are only three different types of rhombic TRP tensegrities for the following reasons. The rhombic truncated cubic and octahedral tensegrities have the same num-bers of bars, strings and nodes, and the connection relations be-tween the elements and the nodes are also identical. This indicates that both the topologies and connectivity matrices of a rhombic truncated cubic tensegrity and a rhombic truncated octa-hedral tensegrity can be expressed in the same form. Therefore, the rhombic truncated cubic and octahedral tensegrities can be re-garded as the same type. For the same reasons, the rhombic trun-cated dodecahedral and icosahedral tensegrities can be incorporated into one type. The structural topologies of the three types of rhombic TRP tensegrities are shown in Fig. 4(a–c), which will be referred to as rhombic tetrahedral, cubic/octahedral, and dodecahedral/icosahedral tensegrities, respectively. According to the topology, the strings in a rhombic TRP tensegrity structure are classified into two types: type-1 and type-2. As can be seen from Fig. 4, each three type-1 strings form a triangle in all rhombic TRP tensegrities, while the type-2 strings form a triangle, a quad-rangle, and a pentagon in rhombic truncated tetrahedral, cubic/octahedral, or dodecahedral/icosahedral tensegrities, respectively. A rhombic cell consists of one bar, two type-1 strings, and two type-2 strings, as shown in Fig. 2(c).

Referring to the Schläfli symbol $\{n, m\}$ for regular polyhedra, we further find that for all rhombic TRP tensegrities, the number of edges in a polygon consisting of type-1 strings, c, equals the smaller

(a)

○ Vertex ━━ Edge

(b)

○ Node ━━ Bar
　　　　　━━ String

(c)

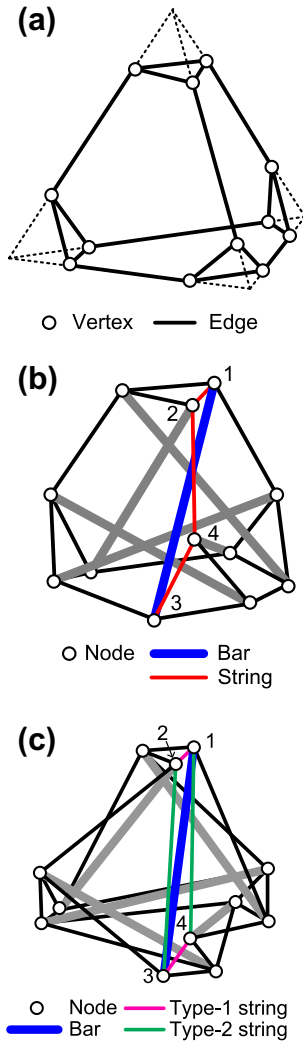○ Node ━━ Type-1 string
━━ Bar ━━ Type-2 string

Fig. 2. (a) The edges and vertices of a truncated tetrahedron, (b) the corresponding Z-based truncated tetrahedral tensegrity, and (c) the corresponding rhombic truncated tetrahedral tensegrity. In (b) and (c), a Z-shaped cell and a rhombic cell are highlighted, respectively, by its nodes 1–4.
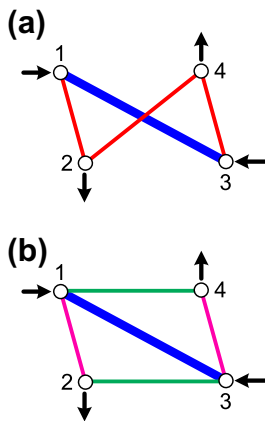
(a)

(b)

Fig. 3. Load-bearing feature of (a) a Z-shaped cell and (b) a rhombic cell. The external forces should be applied in a certain range of direction such that the bar is under compression and the strings are under tension.

number of n and m, that is, $c = \min(n, m) = 3$. In addition, the number of edges in a polygon consisting of type-2 strings, b, is equal to
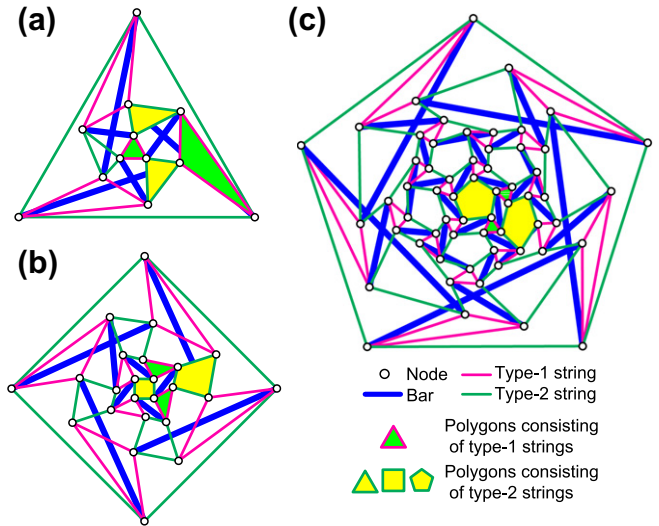
(a)

(b)

(c)

○ Node ━━ Type-1 string
━━ Bar ━━ Type-2 string

△ Polygons consisting of type-1 strings

△ □ ⬠ Polygons consisting of type-2 strings

Fig. 4. Topologies of rhombic truncated (a) tetrahedral, (b) cubic/octahedral, and (c) dodecahedral/icosahedral tensegrities.

the larger of n and m, i.e., $b = \max(n, m) = 3, 4,$ and 5 for rhombic truncated tetrahedral, cubic/octahedral, and dodecahedral/icosahedral tensegrities, respectively. These relations can also be observed from Fig. 4, where two polygons consisting of type-1 strings and two polygons consisting of type-2 strings are highlighted.

3. Self-equilibrium and super-stability of tensegrities

3.1. Self-equilibrium of tensegrities

Let $e(ij)$ designate the element connecting nodes i and j. The force density of an element is defined as the ratio of its internal force $t_{e(ij)}$ to its current length $l_{e(ij)}$ (Schek, 1974):

$$q_{e(ij)} = \frac{t_{e(ij)}}{l_{e(ij)}}. \tag{1}$$

The force density matrix $\mathbf{D} \in \mathbb{R}^{n_n \times n_n}$ of a tensegrity structure, with n_n being the total number of nodes, is determined by the connectivity and force densities of all elements (Vassart and Motro, 1999). Its components D_{ij} are defined as (Zhang et al., 2012)

$$D_{ij} = \begin{cases} -q_{e(ij)} & \text{if } i \neq j \text{ and } i \text{ is connected with } j \text{ by an element,} \\ 0 & \text{if } i \neq j \text{ and } i \text{ does not connect with } j, \\ -\sum_{k \neq j} D_{ik} & \text{if } i = j. \end{cases} \tag{2}$$

In terms of the force density matrix, the structural self-equilibrium conditions can be expressed as (Zhang and Ohsaki, 2012)

$$\mathbf{D} \cdot \mathbf{x} = \mathbf{D} \cdot \mathbf{y} = \mathbf{D} \cdot \mathbf{z} = \mathbf{0}, \tag{3}$$

where $\mathbf{x} \in \mathbb{R}^{n_n \times 1}$, $\mathbf{y} \in \mathbb{R}^{n_n \times 1}$, and $\mathbf{z} \in \mathbb{R}^{n_n \times 1}$ denote the vectors of the x, y, and z coordinates of the nodes from 1 to n_n, respectively.

Only when the force density matrix has at least $d + 1$ zero-eigenvalues, can a self-equilibrated state be solved from Eq. (3), where d is the dimension of the structure (Connelly and Back, 1998; Schenk et al., 2007; Tran and Lee, 2010). The characteristic polynomial of the force density matrix $\mathbf{D} \in \mathbb{R}^{n_n \times n_n}$ is written as

$$\det(\lambda \mathbf{I} - \mathbf{D}) = \lambda^{n_n} + P_{n_n-1}\lambda^{n_n-1} + \cdots + P_3\lambda^3 + P_2\lambda^2 + P_1\lambda + P_0 = 0, \tag{4}$$

where P_k ($k = 0, 1, 2, \ldots, n_n - 1$) are the polynomial functions of the element force densities, $\mathbf{I} \in \mathbb{R}^{n_n \times n_n}$ is the unit matrix, and λ is an

eigenvalue of **D**. In the case when there is no node fixed in a self-equilibrated tensegrity structure, P_0 always equals zero (Tibert and Pellegrino, 2003; Zhang and Ohsaki, 2012; Zhang et al., 2012). In addition, the self-equilibrium of a three-dimensional tensegrity structure (i.e., $d = 3$) requires that (Zhang et al., 2012)

$$P_3 = P_2 = P_1 = 0. \tag{5}$$

The above analysis holds for all three-dimensional tensegrities. As aforementioned, a rhombic TRP tensegrity structure has three types of elements, namely, bars, type-1 strings, and type-2 strings. In this study, the force densities in each type of elements are set as an identical value. More specifically, $q_{e(ij)}$ in the force density matrix **D** are taken as q_b, q_{s1}, and q_{s2} for the bars, type-1 strings, and type-2 strings, respectively. It is clearly known from Eq. (3) that in the absent of external forces, the self-equilibrium of a tensegrity structure depends only on two independent normalized force densities, which may be taken as $Q_1 = -q_{s1}/q_b > 0$ and $Q_2 = -q_{s2}/q_b > 0$, where the negative sign is introduced because the strings should be in tension and the bars should be in compression. Thus, for a rhombic TRP tensegrity structure, the polynomials P_α ($\alpha = 1, 2, 3$) in the self-equilibrium conditions in Eq. (5) can be written as functions of Q_1 and Q_2.

3.2. Super-stability of tensegrities

A tensegrity structure is said to be *super-stable* if it is stable for any level of the self-equilibrium force densities without causing material failure (Connelly and Back, 1998; Juan and Tur, 2008). The super-stability conditions of tensegrities are (Connelly, 1999; Zhang and Ohsaki, 2007; Zhang et al., 2012):

  (i) the bars have negative force densities, and strings have positive force densities,
 (ii) the nullity of the force density matrix is exactly $d + 1$,
(iii) the force density matrix is positive semi-definite, and
(iv) there are no affine (infinitesimal) flexes of the structure, or equivalently, the rank of the structural geometry matrix is $d(d + 1)/2$.

These four conditions ensuring the super-stability of tensegrities have been discussed in details by Zhang and Ohsaki (2007) and Zhang et al. (2012). For rhombic TRP tensegrities, condition (i) can be satisfied by setting $q_b < 0$, $q_{s1} > 0$, and $q_{s2} > 0$. Conditions (ii) and (iii) can be examined via the eigenvalues of the force density matrix, and they will be satisfied when the total number of its zero-eigenvalues is four and the minimum eigenvalue is zero. Condition (iv) can be ensured provided that the rank of the structural geometry matrix defined by Zhang and Ohsaki (2007) is six. In Section 5, we will investigate the super-stability property of rhombic TRP tensegrities by considering the above conditions.

4. Self-equilibrium analysis

In this section, we analyze the self-equilibrium property of rhombic truncated tetrahedral, cubic/octahedral, and dodecahedral/icosahedral tensegrities by invoking the self-equilibrium conditions in Eq. (5).

4.1. Rhombic truncated tetrahedral tensegrities

A rhombic truncated tetrahedral tensegrity has 6 bars, 12 type-1 strings, 12 type-2 strings, and 12 nodes. Thus, its force density matrix is 12×12 in size, whose components can be calculated from Eq. (2). Substituting the obtained force density matrix into Eq. (4), the expressions of P_α ($\alpha = 1, 2, 3$) are solved and given in

Eqs. (A.1), (A.2), (A.3) of Appendix A. Thus, the self-equilibrium condition of rhombic truncated tetrahedral tensegrities reduces to the following equation

$$Q_1^2 Q_2 + Q_1 Q_2^2 - \frac{1}{2}Q_1^2 - \frac{1}{2}Q_2^2 - \frac{4}{3}Q_1 Q_2 + \frac{1}{3}Q_1 + \frac{1}{3}Q_2 = 0. \tag{6}$$

4.2. Rhombic truncated cubic/octahedral tensegrities

A rhombic truncated cubic/octahedral tensegrity has 12 bars, 24 type-1 strings, 24 type-2 strings, and 24 nodes, with a 24×24 force density matrix from Eq. (2). In this case, P_α ($\alpha = 1, 2, 3$) in Eq. (4) are expressed in Eqs. (A.4), (A.5), (A.6) of Appendix A. Combining them with Eq. (5), we obtain the following three equations

$$Q_1 + Q_2 = 0, \tag{7}$$

$$Q_2^2 + \frac{3}{2}Q_1 Q_2 - \frac{3}{4}Q_1 - \frac{3}{4}Q_2 = 0, \tag{8}$$

$$Q_1^2 Q_2 + \frac{2}{3}Q_1 Q_2^2 - \frac{1}{2}Q_1^2 - \frac{1}{3}Q_2^2 - \frac{4}{3}Q_1 Q_2 + \frac{1}{3}Q_1 + \frac{1}{3}Q_2 = 0. \tag{9}$$

Eqs. (7)–(9) cover all self-equilibrated states of rhombic truncated cubic/octahedral tensegrities.

4.3. Rhombic truncated dodecahedral/icosahedral tensegrities

A rhombic truncated dodecahedral/icosahedral tensegrity has 30 bars, 60 type-1 strings, 60 type-2 strings, and 60 nodes, corresponding to a 60×60 force density matrix. In this case, the coefficients P_α ($\alpha = 1, 2, 3$) in Eq. (4) are given in Eqs. (A.7), (A.8), (A.9) of Appendix A. Substituting them into Eq. (5) leads to the following six equations

$$Q_1 + Q_2 = 0, \tag{10}$$

$$Q_2^2 + 2Q_1 Q_2 - Q_1 - Q_2 = 0, \tag{11}$$

$$Q_2^2 + \frac{6}{5}Q_1 Q_2 - \frac{3}{5}Q_1 - \frac{3}{5}Q_2 = 0, \tag{12}$$

$$\begin{aligned}Q_1^3 Q_2 + \frac{5}{9}Q_1 Q_2^3 + \frac{5}{3}Q_1^2 Q_2^2 - \frac{1}{2}Q_1^3 - \frac{5}{18}Q_2^3 - \frac{33}{18}Q_1^2 Q_2 - \frac{29}{18}Q_1 Q_2^2 \\ + \frac{1}{3}Q_1^2 + \frac{1}{3}Q_2^2 + \frac{2}{3}Q_1 Q_2 = 0,\end{aligned} \tag{13}$$

$$Q_1^2 Q_2 + \frac{5+\sqrt{5}}{6}Q_1 Q_2^2 - \frac{1}{2}Q_1^2 - \frac{5+\sqrt{5}}{12}Q_2^2 - \frac{4}{3}Q_1 Q_2 + \frac{1}{3}Q_1 + \frac{1}{3}Q_2 = 0, \tag{14}$$

$$Q_1^2 Q_2 + \frac{5-\sqrt{5}}{6}Q_1 Q_2^2 - \frac{1}{2}Q_1^2 - \frac{5-\sqrt{5}}{12}Q_2^2 - \frac{4}{3}Q_1 Q_2 + \frac{1}{3}Q_1 + \frac{1}{3}Q_2 = 0. \tag{15}$$

All self-equilibrated states of rhombic truncated dodecahedral/icosahedral tensegrities can be solved from Eqs. (10)–(15).

5. Super-stability analysis

In Section 4, all self-equilibrium solutions of the three types of rhombic TRP tensegrities have been derived. However, it is worth pointing out that some of them satisfy the super-stability conditions while the others do not. In this section, therefore, we will further examine the conditions (i)–(iv) of super-stability given in Section 3.2, in conjunction with the self-equilibrium solutions in Section 4. The results will provide a basis for establishing the necessary and sufficient condition for the self-equilibrium and super-stability of rhombic TRP tensegrities.

Firstly, condition (i) for the super-stability of a rhombic TRP tensegrity structure requires that $q_b < 0$, $q_{s1} > 0$, and $q_{s2} > 0$. Thus the normalized force densities in Eqs. (6)–(15) must be positive, i.e., $Q_1 = -q_{s1}/q_b > 0$ and $Q_2 = -q_{s2}/q_b > 0$, indicating that Eqs. (7) and (10) should be ruled out for super-stable tensegrities.

Secondly, condition (ii) requires that the force density matrix solved from the self-equilibrium solutions has exactly four zero-eigenvalues. We substitute the force densities determined by Eqs. (11)–(13) into Eq. (4) and find that $P_4 = 0$ for rhombic truncated dodecahedral/icosahedral tensegrities. This indicates that each force density matrix satisfying these equations has at least five zero-eigenvalues and thus cannot produce super-stable tensegrities. Therefore, Eqs. (11)–(13) will not be considered in the super-stability analysis in what follows.

Thirdly, condition (iii) demands that the force density matrix solved from the self-equilibrium solutions should be positive semi-definite. However, our calculation shows that the minimum eigenvalue of all force density matrices solved from Eqs. (8) and (14) are always negative provided that $Q_1 > 0$ and $Q_2 > 0$, as shown in Fig. 5. In this figure, Eq. (8) corresponds to only one curve while Eq. (14) has two branches. Hence, Eqs. (8) and (14) cannot meet condition (iii) for super-stable tensegrities.

According to the above analysis, Eqs. (7), (8), (10), and (11)–(14) should be excluded in the super-stability analysis of rhombic TRP tensegrities. Therefore, it is only possible to seek the super-stable states of rhombic truncated tetrahedral, cubic/octahedral, and dodecahedral/icosahedral tensegrities from Eqs. (6), (9), and (15), respectively. The Q_1–Q_2 curves of Eqs. (6), (9), and (15) are shown

in Fig. 6, each of which has three branch curves numbered by 1, 2, and 3, respectively. For the self-equilibrated states on the curves in Fig. 6, it is clear that Curve-1 and part of Curve-2 are not in the region $Q_1 > 0$ and $Q_2 > 0$ and thus violate condition (i). All force density matrices corresponding to Curve-2 in $Q_1 > 0$ and $Q_2 > 0$ have negative eigenvalues, as shown in Fig. 7, and thus cannot meet condition (iii). This means that Curve-1 and Curve-2 cannot produce super-stable states. However, the force densities in Curve-3 are always in the region $Q_1 > 0$ and $Q_2 > 0$, and the corresponding force density matrices are all positive semi-definite and have exactly four zero-eigenvalues. Therefore, Curve-3 satisfies conditions (i)–(iii).

Finally, we check the rank of the structural geometry matrix defined by Zhang and Ohsaki (2007) in order to ensure the satisfaction of super-stability condition (iv). As analyzed above, among all self-equilibrium solutions in Section 4, only the branch Curve-3 of Eqs. (6), (9), and (15) can satisfy conditions (i)–(iii) of super-stability. Thus condition (iv) is checked only for Curve-3. Our calculations demonstrate that all structural geometry matrices corresponding to Curve-3 have a rank of six, meeting condition (iv). Therefore, the solutions on Curve-3 satisfy all four conditions of super-stability given in Section 3.2.

Thus, it becomes clear that for the self-equilibrium solutions obtained in Section 4, only the solutions of Eqs. (6), (9), and (15) in the region $Q_1 = -q_{s1}/q_b > 1/2$ and $Q_2 = -q_{s2}/q_b > 1/2$ with $q_b < 0$ can satisfy both the self-equilibrium and super-stability conditions. As we will show in Section 6, these self-equilibrated and super-stable states of rhombic TRP tensegrities can be further formulated in a unified expression.

6. Unified solution for self-equilibrium and super-stability

In this section, we will establish a unified and closed-form solution for the necessary and sufficient condition of all rhombic TRP tensegrities. Inspired by the results in Section 4, the unified solution will be expressed in a polynomial form, with the coefficients solved from several special equilibrated states. Then the necessary and sufficient condition that ensures the existence of self-equilibrated and super-stable states will be established.

6.1. Unified form

Based on the analyses in Sections 4 and 5, we will establish a unified closed-form solution for the self-equilibrated and super-stable states of all rhombic TRP tensegrities. By directly solving the self-equilibrium conditions and examining the super-stability conditions, we have individually derived the self-equilibrium and super-stability solutions of rhombic truncated tetrahedral, cubic/octahedral, and dodecahedral/icosahedral tensegrities, which are given in Eqs. (6), (9), and (15), respectively. The three equations can be rewritten as

$$\left(Q_2 - \frac{1}{2}\right)Q_1^2 + \left(Q_1 - \frac{1}{2}\right)Q_2^2 - \frac{4}{3}Q_1Q_2 + \frac{1}{3}Q_1 + \frac{1}{3}Q_2 = 0, \quad (16)$$

$$\left(Q_2 - \frac{1}{2}\right)Q_1^2 + \frac{2}{3}\left(Q_1 - \frac{1}{2}\right)Q_2^2 - \frac{4}{3}Q_1Q_2 + \frac{1}{3}Q_1 + \frac{1}{3}Q_2 = 0, \quad (17)$$

$$\left(Q_2 - \frac{1}{2}\right)Q_1^2 + \frac{5-\sqrt{5}}{6}\left(Q_1 - \frac{1}{2}\right)Q_2^2 - \frac{4}{3}Q_1Q_2 + \frac{1}{3}Q_1 + \frac{1}{3}Q_2$$
$$= 0, \quad (18)$$

respectively. It is seen that Eqs. (16)–(18) can be unified in the following form:

$$\left(Q_2 - \frac{1}{2}\right)Q_1^2 + A\left(Q_1 - \frac{1}{2}\right)Q_2^2 - \frac{4}{3}Q_1Q_2 + \frac{1}{3}Q_1 + \frac{1}{3}Q_2 = 0, \quad (19)$$
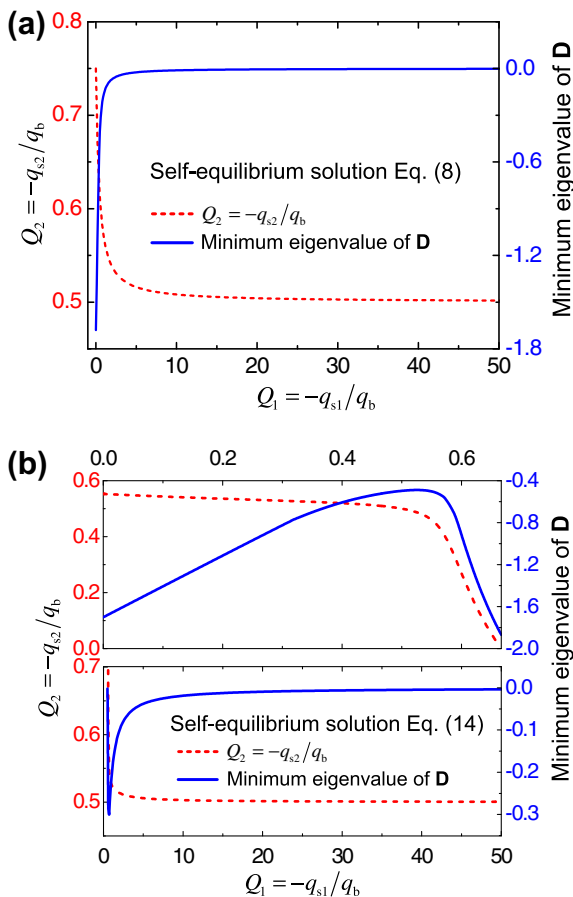

Fig. 5. Self-equilibrium solutions violating the positive semi-definite condition of super-stability for rhombic truncated (a) cubic/octahedral and (b) dodecahedral/icosahedral tensegrities.
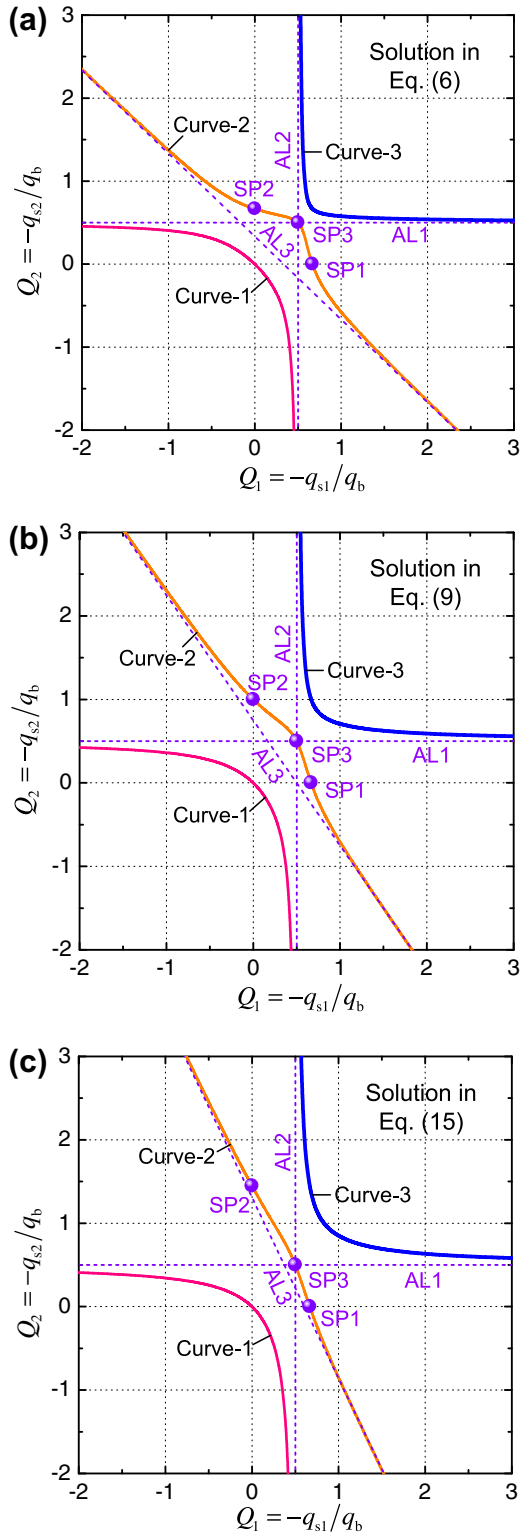
Fig. 6. Self-equilibrium solutions for rhombic truncated (a) tetrahedral, (b) cubic/octahedral, and (c) dodecahedral/icosahedral tensegrities. Only the self-equilibrated states in Curve-3 are super-stable.
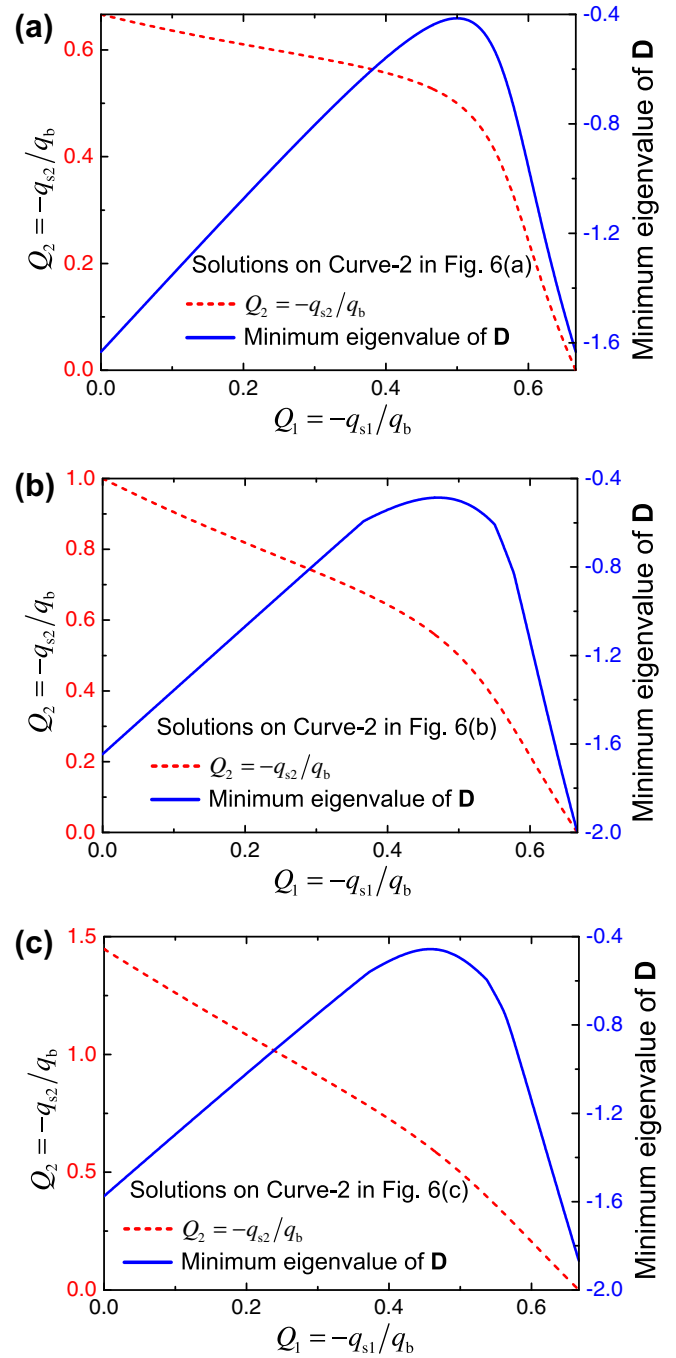

Fig. 7. Self-equilibrium solutions corresponding to Curve-2 in Fig. 6 in the region of $Q_1 > 0$ and $Q_2 > 0$ for rhombic truncated (a) tetrahedral, (b) cubic/octahedral, and (c) dodecahedral/icosahedral tensegrities.

$$(Q_2 - a_1)Q_1^2 + A(Q_1 - a_2)Q_2^2 - a_3 Q_1 Q_2 + a_4 Q_1 + a_5 Q_2 = 0, \qquad (20)$$

where a_β ($\beta = 1, 2, 3, 4, 5$) are all constant and their values will be solved below.

In what follows, we will determine A and a_β ($\beta = 1, 2, 3, 4, 5$) from six special self-equilibrated states of rhombic TRP tensegrities, which correspond to three asymptotic lines (i.e., AL1, AL2, and AL3) and three special points (i.e., SP1, SP2, and SP3) on the $Q_1 - Q_2$ curves of Eqs. (6), (9), and (15), as shown in Fig. 6. Once A and a_β are determined, a unified solution for the self-equilibrium and super-stability of all rhombic TRP tensegrities will be obtained.

demonstrating that for all types of rhombic TRP tensegrities, the self-equilibrated and super-stable states can be captured by a unified solution containing only one parameter A with a value depending on the structural type. To further verify this finding and determine the expression of A, Eq. (19) is recast as

6.1.1. Coefficients a_1 and a_2

First, we solve the coefficients a_1 and a_2 in Eq. (20) from the self-equilibrated states corresponding to the asymptotic lines AL1 and AL2. The force density of an element, defined as the ratio of its internal force to its current length, approaches infinite when the element length approaches zero. For each type of rhombic TRP tensegrities, two special self-equilibrated states, AL1 and AL2, can be defined, as shown in Fig. 6. In the former, all type-1 strings are of infinitesimal length, and thus their force density is infinite, that is, $Q_1 = -q_{s1}/q_b \to \infty$. In the latter, all type-2 strings are of infinitesimal length and then their force density is infinite, that is $Q_2 = -q_{s2}/q_b \to \infty$. Take rhombic truncated cubic/octahedral tensegrities as an example. Fig. 8(a) and (b) show the AL1 and AL2 configurations, which have the shapes of a regular cube and a regular octahedron, respectively.

At the self-equilibrated state AL1, all type-1 strings have an infinitesimal length (i.e., $Q_1 \to \infty$), and thus the bar and the two type-2 strings in each rhombic cell will be aligned and have the same length, as shown in the dashed box in Fig. 8(a). Each cell will be in self-equilibrium itself as the force densities of the bars and type-2 strings satisfy $Q_2 = -q_{s2}/q_b = 1/2$. Correspondingly, the configuration assembled by these rhombic cells must be self-equilibrated. For all types of rhombic TRP tensegrities approaching the AL1 state, therefore, the values of $Q_1 \to \infty$ and $Q_2 = 1/2$ must satisfy the self-equilibrium solution in Eq. (20).

Analogously, at the self-equilibrated state AL2, the bar and the two type-1 strings in each rhombic cell are aligned and have the same length since the two type-2 strings have the zero length and $Q_2 \to \infty$, as shown in Fig. 8(b). In this case, each cell will be self-equilibrated itself as $Q_1 = -q_{s1}/q_b = 1/2$. Thus, for all rhombic TRP tensegrities approaching the AL2 state, the self-equilibrium solution in Eq. (20) always has the solution of $Q_1 = 1/2$ and $Q_2 \to \infty$.

Rewrite Eq. (20) as

$$(Q_2 - a_1) + A(Q_1 - a_2)\frac{Q_2^2}{Q_1^2} - a_3\frac{Q_2}{Q_1} + a_4\frac{1}{Q_1} + a_5\frac{Q_2}{Q_1^2} = 0, \qquad (21)$$

$$(Q_2 - a_1)\frac{Q_1^2}{Q_2^2} + A(Q_1 - a_2) - a_3\frac{Q_1}{Q_2} + a_4\frac{Q_1}{Q_2^2} + a_5\frac{1}{Q_2} = 0. \qquad (22)$$

Substituting $(Q_1 \to \infty, Q_2 = 1/2)$ into Eq. (21) and $(Q_1 = 1/2, Q_2 \to \infty)$ into Eq. (22), we get

$$a_1 = \frac{1}{2}, \qquad (23)$$

$$a_2 = \frac{1}{2}. \qquad (24)$$

6.1.2. Coefficient a_4

To determine the coefficient a_4, we consider the special self-equilibrated state, SP1, in which all type-2 strings have the zero force density (i.e., $Q_2 = -q_{s2}/q_b = 0$) and thus can be eliminated without affecting the equilibrium and shape of the structures (Li et al., 2010b). In this state, we denote the force densities of the bars and the type-1 strings as $\bar{q}_b$ and $\bar{q}_{s1}$, respectively. For illustration, Fig. 8(c) shows a rhombic cubic/octahedral tensegrity at the self-equilibrated state SP1.

If all type-2 strings have been removed, there will be only one bar and two type-1 strings left at each node, and the three elements must lie in the same plane as a requirement of force equilibrium (Motro, 2003). Furthermore, the structural symmetry requires that the solid centers of the structure, the midpoints of all bars, and the centers of all polygons consisting of type-1 strings
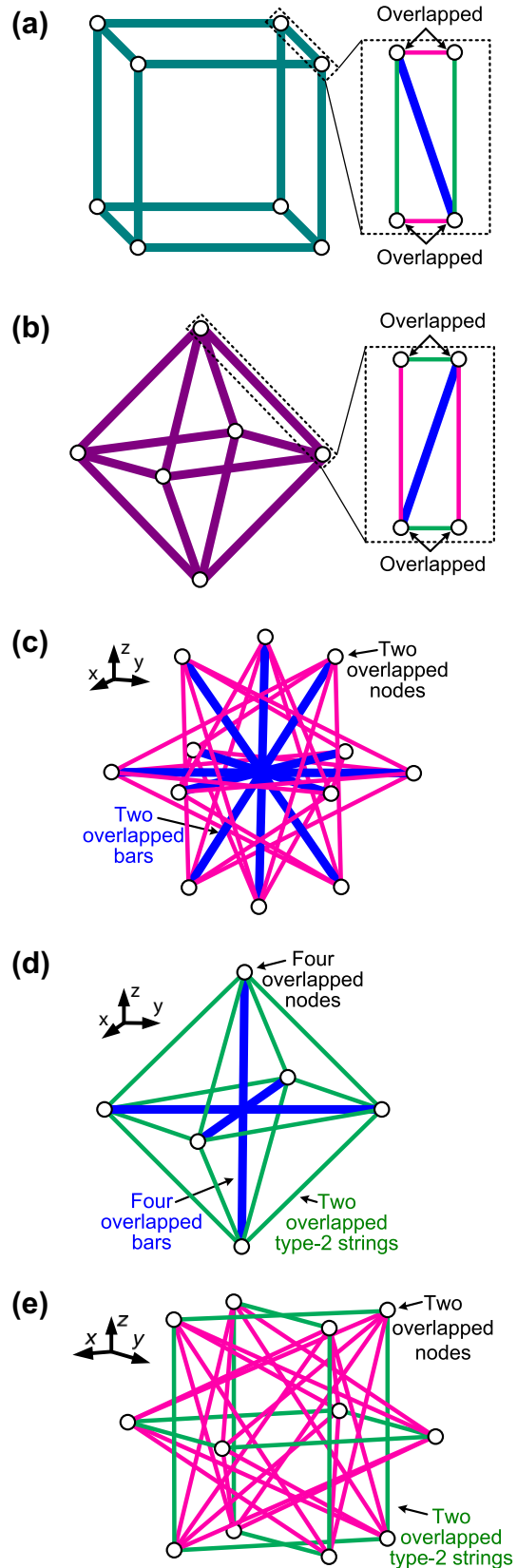

Fig. 8. Several special self-equilibrated configurations of rhombic truncated cubic/octahedral tensegrities with (a) the type-1 strings of infinitesimal length, (b) the type-2 strings of infinitesimal length, (c) the type-2 strings of zero force density, (d) the type-1 strings of zero force density, and (e) the bars of zero force density.

should be overlapped. Thus, any node and its three connecting nodes must lie on a circle with center located at the midpoint of the bar jointed to it. Then for a specified node R, we establish a local Cartesian coordinate system $(O - xy)$, as shown in Fig. 9(a), where the origin O is located at the center of the circle, and the x- and y-axes are parallel and perpendicular to the bar, respectively. The nodes connected to the node R via two type-1 strings are numbered as 1 and 2, and the node connected to R via the bar is numbered as 3. The force equilibrium condition at the node R in the x-direction reads

$$\bar{q}_{s1}(x_1 - x_R) + \bar{q}_{s1}(x_2 - x_R) + \bar{q}_b(x_3 - x_R) = 0. \quad (25)$$

Set the radius of the circle (or the length of the bar) as unit length. Then the nodal x-coordinates are $x_R = 1$, $x_1 = x_2 = -\cos(2\pi/c)$ and $x_3 = -1$, where $c = \min(n, m)$ is the total number of edges in each polygon consisting of type-1 strings. Substituting the nodal coordinates into Eq. (25), one obtains

$$\bar{Q}_1 = -\frac{\bar{q}_{s1}}{\bar{q}_b} = \left(1 - \cos\frac{2\pi}{c}\right)^{-1} = \frac{2}{3}. \quad (26)$$

Therefore, for all types of rhombic TRP tensegrities, the location of SP1 in the $Q_1 - Q_2$ curves is identical and located at $(Q_1 = 2/3, Q_2 = 0)$.

Combining Eq. (26) and $Q_2 = 0$ with (20) results in

$$a_4 = \frac{1}{2}\left(1 - \cos\frac{2\pi}{c}\right)^{-1} = \frac{1}{3}, \quad (27)$$

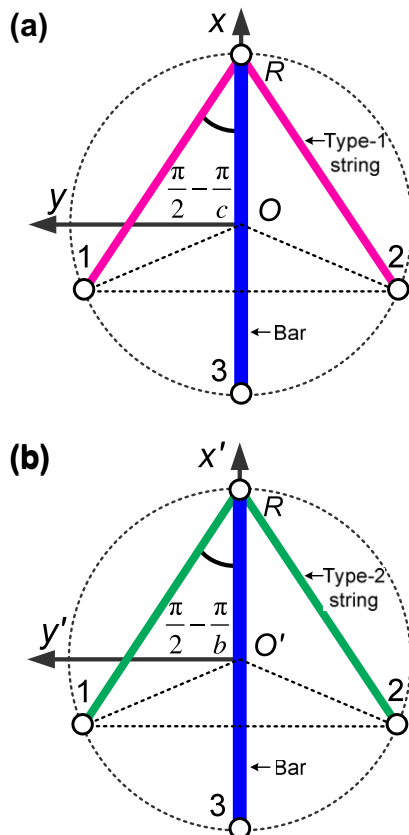where $c = \min(n, m) = 3$ for all rhombic TRP tensegrities.

Fig. 9. A generic node R in the self-equilibrated rhombic TRP tensegrities with (a) the type-2 strings of zero force density, and (b) the type-1 strings of zero force density. In each figure, the two strings and 1 bar connected to the node R are coplanar.

6.1.3. Coefficients A and a_5

To solve the expressions of A and a_5, two special self-equilibrated states are considered, that is, SP2 with $q_{s1} = 0$ and AL3 with $q_b = 0$. In SP2, all type-1 strings can be removed, while in AL3, all bars can be removed (Li et al., 2010b). It is emphasized that AL3 is a self-equilibrated but unstable state, in which either the type-1 or type-2 strings will be in compression. For illustration, the SP2 and AL3 configurations of rhombic truncated cubic/octahedral tensegrities are shown in Fig. 8(d) and (e), respectively.

At the self-equilibrated state SP2, the type-1 strings are of zero force density and thus $Q_1 = -q_{s1}/q_b = 0$. In this state, the force densities of the bars and type-2 strings are denoted as $\tilde{q}_b$ and $\tilde{q}_{s2}$, respectively. Analogous to the analysis in Section 6.1.2, the SP2 configuration with all type-1 strings having been removed is analyzed as follows. As shown in Fig. 9(b), nodes 1 and 2 are connected with a specified node R by two type-2 strings, and node 3 is jointed to R by one bar. Refer to a local Cartesian coordinate system $(O' - x'y')$, where the origin O' is at the midpoint of the bar, and the x' and y' axes are parallel and perpendicular to the bar, respectively. Set the radius of the circle as unit length. Then the nodal x'-coordinates are $x'_R = 1, x'_1 = x'_2 = -\cos(2\pi/b)$, and $x'_3 = -1$, where $b = \max(n, m)$ is the total number of edges in each polygon consisting of type-2 strings. The force equilibrium condition at the node R in the x'-direction gives

$$\tilde{q}_{s2}(x'_1 - x'_R) + \tilde{q}_{s2}(x'_2 - x'_R) + \tilde{q}_b(x'_3 - x'_R) = 0. \quad (28)$$

Substituting the coordinates of nodes R, 1, 2, and 3 into Eq. (28), we obtain

$$\tilde{Q}_2 = -\frac{\tilde{q}_{s2}}{\tilde{q}_b} = \left(1 - \cos\frac{2\pi}{b}\right)^{-1}. \quad (29)$$

Thus the location of SP2 in the $Q_1 - Q_2$ curve is determined as $(Q_1 = 0, Q_2 = [1 - \cos(2\pi/b)]^{-1})$.

Combining $Q_1 = 0$ and Eq. (29) with Eq. (20) leads to

$$A = 2\left(1 - \cos\frac{2\pi}{b}\right)a_5. \quad (30)$$

At the self-equilibrated state AL3, the structural self-equilibrium condition requires that either the type-1 or type-2 strings are under compression. This fictitious self-equilibrated stated is allowed only for the sake of calculations. For simplicity and without loss of generality, the type-2 strings are specified to have a negative force density in the following analysis. We denote the slope of the $Q_1 - Q_2$ curve at the limit state of AL3 in Fig. 6 as

$$s = \lim_{\substack{Q_1 \to +\infty \\ Q_2 \to -\infty}} \frac{Q_2}{Q_1}. \quad (31)$$

Rewrite Eq. (20) as

$$\left(1 - \frac{a_1}{Q_2}\right) + A\left(1 - \frac{a_2}{Q_1}\right)\frac{Q_2}{Q_1} - a_3\frac{1}{Q_1} + a_4\frac{1}{Q_1 Q_2} + a_5\frac{1}{Q_1^2} = 0. \quad (32)$$

Then from the limit state of $(Q_1 \to +\infty, Q_2 \to -\infty)$, we get

$$A = -\frac{1}{s}. \quad (33)$$

As all bars have been removed at the AL3 state, there are only two type-1 strings and two type-2 strings at each node. Let $\hat{q}_{s1}$ and $\hat{q}_{s2}$ respectively denote the force densities of the type-1 and type-2 strings in this special case. According to the analysis of force equilibrium at a specified node in the self-equilibrated states SP1 ($q_{s2} = 0$) and SP2 ($q_{s1} = 0$), we will solve the nodal force equilibrium at the AL3 state ($q_b = 0$) as follows.

From the analysis in Section 6.1.2, we have known that at the SP1 state, Eq. (25) can ensure the equilibrium at all nodes if

$\bar{q}_{s1} = [1 - \cos(2\pi/c)]^{-1}$ and $\bar{q}_b = -1$. In addition, it is seen from Eq. (28) that at the SP2 state, all nodes will be in equilibrium when $\tilde{q}_{s2} = [1 - \cos(2\pi/b)]^{-1}$ and $\tilde{q}_b = -1$. Thus, the AL3 state should be self-equilibrated when the force densities of the type-1 strings and type-2 strings are specified as $\hat{q}_{s1} = \bar{q}_{s1}$ and $\hat{q}_{s2} = -\tilde{q}_{s2}$ while the force density of the bars is $\bar{q}_b - \tilde{q}_b = 0$. This solution can be further verified by checking the self-equilibrium conditions in Eq. (5).

Thus s can be solved from Eq. (31) as

$$s = \lim_{\substack{Q_1 \to +\infty \\ Q_2 \to -\infty}} \frac{Q_2}{Q_1} = \frac{\hat{q}_{s2}}{\hat{q}_{s1}} = -\left(1 - \cos\frac{2\pi}{c}\right)\left(1 - \cos\frac{2\pi}{b}\right)^{-1}. \quad (34)$$

Substituting Eq. (34) into Eq. (33) leads to

$$A = \left(1 - \cos\frac{2\pi}{c}\right)^{-1}\left(1 - \cos\frac{2\pi}{b}\right) = \frac{2}{3}\left(1 - \cos\frac{2\pi}{b}\right). \quad (35)$$

Comparing Eq. (35) with Eq. (30), the parameter a_5 is determined as

$$a_5 = \frac{1}{2}\left(1 - \cos\frac{2\pi}{c}\right)^{-1} = \frac{1}{3}. \quad (36)$$

6.1.4. Coefficient a_3

Finally, the coefficient a_3 is determined by invoking another special self-equilibrated state, SP3. As we will show below, it is always located at the point $(Q_1 = 1/2, Q_2 = 1/2)$ in the $Q_1 - Q_2$ curve for all rhombic TRP tensegrity structures, as shown in Fig. 6. At this special state, all type-1 and type-2 strings have the same force density, denoted as $\bar{\bar{q}}_{s1} = \bar{\bar{q}}_{s2} = \bar{\bar{q}}_s$. In addition, we denote the force density of the bars as $\bar{\bar{q}}_b$.

Fig. 10(a) shows a planar X-frame tensegrity consisting of two bars and four strings. We find that a rhombic TRP tensegrity structure at the SP3 state can be regarded as an assembly of a certain number of such X-frame tensegrities. Therefore, the rhombic TRP tensegrities will be self-equilibrated provided that all its X-frame sub-structures are in self-equilibrium. For illustration, the SP3 configuration of rhombic truncated tetrahedral tensegrities is shown in Fig. 10(b).

In the assembly, the bars in each two X-frame sub-structures overlaps each other. In the X-frame sub-structures, therefore, the force density of the bars should be $\bar{\bar{q}}_b/2$. Then the self-equilibrium analysis of a X-frame tensegrity gives (Tibert and Pellegrino, 2003)

$$\bar{\bar{q}}_b/2 + \bar{\bar{q}}_s = 0 \quad (37)$$

which can ensure the self-equilibrium of the assembled rhombic TRP structure.

It is known from Eq. (37) that

$$\bar{\bar{Q}}_1 = \bar{\bar{Q}}_2 = -\frac{\bar{\bar{q}}_s}{\bar{\bar{q}}_b} = \frac{1}{2}, \quad (38)$$

dictating the location of SP3 at $(Q_1 = 1/2, Q_2 = 1/2)$ in the $Q_1 - Q_2$ curves for all types of rhombic TRP tensegrities. This self-equilibrated state can be further confirmed by using the self-equilibrium conditions in Eq. (5).

Substituting Eqs. (23), (24), (27), (35), (36), and (38) into (20), one obtains

$$a_3 = \left(\frac{1}{2} - a_1\right) + A\left(\frac{1}{2} - a_2\right) + 2a_4 + 2a_5 = \frac{4}{3}. \quad (39)$$

6.2. Unified solution

With the determination of all coefficients in the unified solution in Eq. (20), it is seen from Eqs. (23), (24), (27), (36), and (39) that a_β
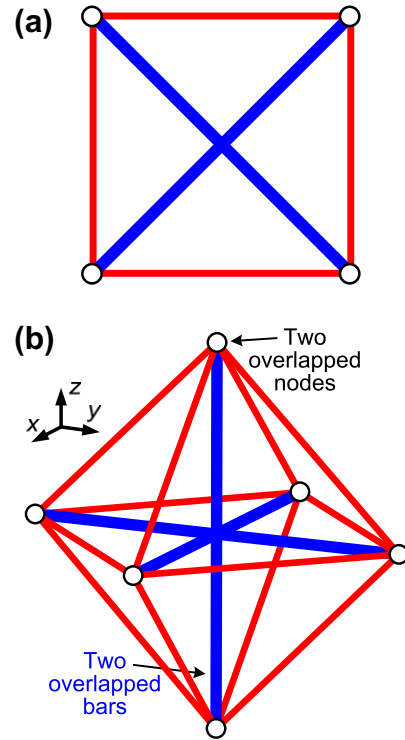

Fig. 10. (a) A self-equilibrated X-frame tensegrity, and (b) a self-equilibrated configuration of rhombic truncated tetrahedral tensegrities, in which the force densities of the bars, type-1 strings, and type-2 strings are assumed to have the relation $q_b:q_{s1}:q_{s2} = -2:1:1$.

($\beta = 1, 2, 3, 4, 5$) are constant for all types of rhombic TRP tensegrities, while the parameter A solved in Eq. (35) depends only upon the polyhedral type. The super-stability analysis in Section 5 enables us to establish the following necessary condition for the self-equilibrated and super-stable states of rhombic TRP tensegrities.

Theorem 1. For all self-equilibrated and super-stable states of rhombic TRP tensegrities, the force densities of elements must satisfy the relation

$$\left(Q_2 - \frac{1}{2}\right)Q_1^2 + \frac{2}{3}\left(1 - \cos\frac{2\pi}{b}\right)\left(Q_1 - \frac{1}{2}\right)Q_2^2 - \frac{4}{3}Q_1 Q_2 + \frac{1}{3}Q_1 + \frac{1}{3}Q_2 = 0, \quad (40)$$

where $Q_1 = -q_{s1}/q_b$, $Q_2 = -q_{s2}/q_b$, and $b = \max(n, m)$ follows the definition of Schläfli symbol $\{n, m\}$ for the corresponding regular polyhedron, with q_b, q_{s1}, and q_{s2} being the force densities of the bars, type-1 strings, and type-2 strings, respectively.

It can be readily verified that the proposed unified solution in Eq. (40) covers all super-stability solutions derived in Section 4. Furthermore, the analysis in Section 5 has shown that only the branch Curve-3 of the above solution in the $Q_1 - Q_2$ diagram in Fig. 6 can satisfy both the self-equilibrium and super-stability conditions. By using the solution in Eq. (40), the force densities on Curve-3 can also be expressed in a unified form. Rewrite Eq. (40) in the quadratic form

$$\frac{2}{3}\left(1 - \cos\frac{2\pi}{b}\right)\left(Q_1 - \frac{1}{2}\right)Q_2^2 + \left(Q_1^2 - \frac{4}{3}Q_1 + \frac{1}{3}\right)Q_2 - \left(\frac{1}{2}Q_1^2 - \frac{1}{3}Q_1\right) = 0. \quad (41)$$

Eq. (41) has two roots, and Curve-3 in Fig. 6 corresponds to the following root:

$$Q_2 = \frac{\sqrt{(3Q_1^2 - 4Q_1 + 1)^2 + 2Q_1(6Q_1^2 - 7Q_1 + 2)(1 - \cos\frac{2\pi}{b})} - (3Q_1^2 - 4Q_1 + 1)}{2(2Q_1 - 1)(1 - \cos\frac{2\pi}{b})}, \quad (42)$$
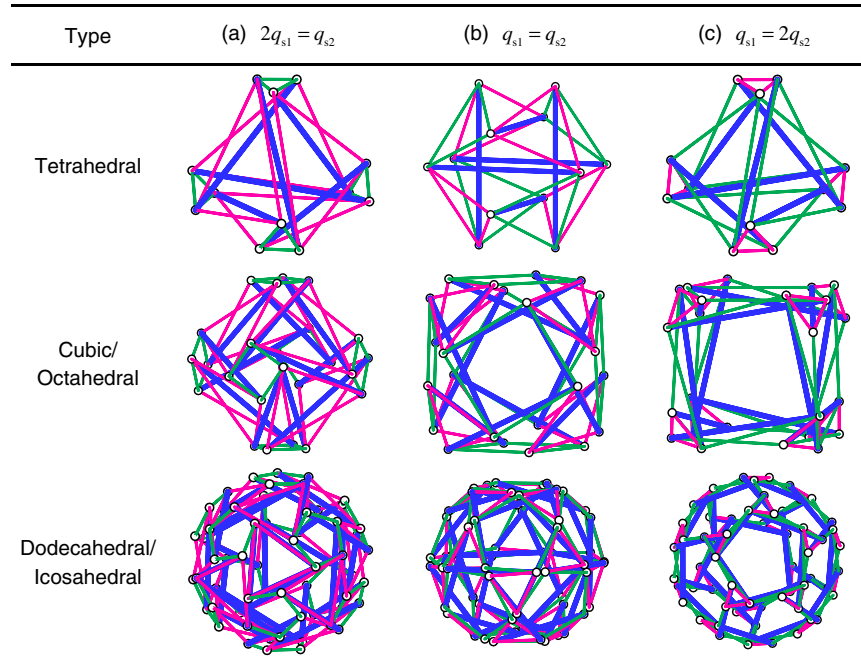
Type	(a) $2q_{s1} = q_{s2}$	(b) $q_{s1} = q_{s2}$	(c) $q_{s1} = 2q_{s2}$
Tetrahedral			
Cubic/ Octahedral			
Dodecahedral/ Icosahedral			

Fig. 11. Some representative self-equilibrated and super-stable configurations of rhombic TRP tensegrities. Here, the force density of the bars is set as $q_b = -1$, and the force densities of the type-1 and type-2 strings are taken as (a) $2q_{s1} = q_{s2}$, (b) $q_{s1} = q_{s2}$, and (c) $q_{s1} = 2q_{s2}$.

where $Q_1 = -q_{s1}/q_b > 1/2$ and $q_b < 0$. Therefore, the necessary and sufficient condition for the self-equilibrated and super-stable states of rhombic TRP tensegrities can be stated as

Theorem 2. A rhombic TRP tensegrity structure is self-equilibrated and super-stable if and only if the force densities of its elements satisfy the relation

$$Q_2 = \frac{\sqrt{(3Q_1^2 - 4Q_1 + 1)^2 + 2Q_1(6Q_1^2 - 7Q_1 + 2)(1 - \cos\frac{2\pi}{b})} - (3Q_1^2 - 4Q_1 + 1)}{2(2Q_1 - 1)(1 - \cos\frac{2\pi}{b})},$$

(43)

where $Q_2 = -q_{s2}/q_b$, $Q_1 = -q_{s1}/q_b > 1/2$, $q_b < 0$, and $b = 3, 4, 5$ for rhombic truncated tetrahedral, cubic/octahedral, dodecahedral/icosahedral tensegrities.

6.3. Self-equilibrated and super-stable configurations

All self-equilibrated and super-stable configurations of rhombic truncated tetrahedral, cubic/octahedral, and dodecahedral/icosahedral tensegrities can be solved from the unified solution in Eq. (43). Some representative examples are shown in Fig. 11(a–c), in which the force density of the bars is set as $q_b = -1$ and the force densities of the strings are $2q_{s1} = q_{s2}$, $q_{s1} = q_{s2}$, and $q_{s1} = 2q_{s2}$, respectively.

It can be seen from Fig. 11 that the self-equilibrated configurations of rhombic TRP tensegrities vary with the ratio of the force densities of the strings, q_{s1}/q_{s2}. The three tensegrities in Fig. 11(a), where $2q_{s1} = q_{s2}$, have the shapes like a truncated tetrahedron, octahedron, and icosahedron, respectively (see Fig. 1b). However, the three tensegrities in Fig. 11(c), where $q_{s1} = 2q_{s2}$, look more like the corresponding dual-pairs, i.e., the truncated tetrahedron, cube, and dodecahedron, respectively (see Fig. 1b). When all type-1 and type-2 strings have the same force density, i.e., $q_{s1} = q_{s2}$, the tensegrities are in an intermediate state, as shown in Fig. 11(b). The configuration of a rhombic truncated tetrahedral tensegrity

with $q_{s1} = q_{s2}$ is also known as an expandable octahedron tensegrity, and the corresponding element force densities solved from Eq. (43) are $Q_{s1} = -q_{s1}/q_b = Q_{s2} = -q_{s2}/q_b = 2/3$, in consistency with the results in the literature (e.g. Koohestani, 2012; Li et al., 2010b; Tibert and Pellegrino, 2003). In addition, it is worth mentioning that the expandable octahedron tensegrity and other rhombic TRP tensegrities has a variety of applications in, for instance, theoretical modeling of cytoskeleton (Ingber, 2010). The unified solution obtained in the present paper is helpful not only for the design of self-equilibrated and super-stable rhombic TRP tensegrities but also for their practical applications.

7. Conclusions

In this paper, we have proposed a unified analytical solution for the self-equilibrium and super-stability of all types of rhombic TRP tensegrities. The simple unified solution allows us to determine their self-equilibrated and super-stable configurations very easily. The necessary and sufficient condition for the self-equilibrated and super-stable rhombic TRP tensegrities is also given. We hope the present work will stimulate further effort directed towards understanding the properties of tensegrities and their applications in biomechanical, civil, and aerospace engineering.

Appendix A. Polynomials P_1, P_2, and P_3

For rhombic truncated tetrahedral tensegrities, the polynomials P_α ($\alpha = 1, 2, 3$) defined in Eq. (4) are

$$P_1 = -576P_{1,4}\left[6(Q_1^2 Q_2 + Q_1 Q_2^2) - 3(Q_1^2 + Q_2^2) - 8Q_1 Q_2 + 2(Q_1 + Q_2)\right]^3, \quad (A.1)$$

$$P_2 = 48P_{2,4}\left[6(Q_1^2Q_2 + Q_1Q_2^2) - 3(Q_1^2 + Q_2^2) - 8Q_1Q_2 + 2(Q_1 + Q_2)\right]^2, \quad (A.2)$$

$$P_3 = -4P_{3,4}\left[6(Q_1^2Q_2 + Q_1Q_2^2) - 3(Q_1^2 + Q_2^2) - 8Q_1Q_2 + 2(Q_1 + Q_2)\right], \quad (A.3)$$

where $P_{1,4}$, $P_{2,4}$, and $P_{3,4}$ are lengthy polynomials, with the second index 4 indicating a truncated tetrahedral tensegrity. The specific expressions of $P_{1,4}$, $P_{2,4}$, and $P_{3,4}$ do not affect structural self-equilibrium conditions and thus are omitted in the present paper.

For rhombic truncated cubic/octahedral tensegrities, P_α ($\alpha = 1, 2, 3$) are

$$P_1 = -9216P_{1,6}(Q_1 + Q_2)^3(4Q_2^2 + 6Q_1Q_2 - 3Q_1 - 3Q_2)^3$$
$$\times (6Q_1^2Q_2 + 4Q_1Q_2^2 - 3Q_1^2 - 2Q_2^2 - 8Q_1Q_2 + 2Q_1 + 2Q_2)^3, \quad (A.4)$$

$$P_2 = 768P_{2,6}(Q_1 + Q_2)^2(4Q_2^2 + 6Q_1Q_2 - 3Q_1 - 3Q_2)^2$$
$$\times (6Q_1^2Q_2 + 4Q_1Q_2^2 - 3Q_1^2 - 2Q_2^2 - 8Q_1Q_2 + 2Q_1 + 2Q_2)^2, \quad (A.5)$$

$$P_3 = -64P_{3,6}(Q_1 + Q_2)(4Q_2^2 + 6Q_1Q_2 - 3Q_1 - 3Q_2)$$
$$\times (6Q_1^2Q_2 + 4Q_1Q_2^2 - 3Q_1^2 - 2Q_2^2 - 8Q_1Q_2 + 2Q_1 + 2Q_2), \quad (A.6)$$

where the specific expressions of $P_{1,6}$, $P_{2,6}$, and $P_{3,6}$ are omitted, and the second index 6 indicates a rhombic truncated cubic/octahedral tensegrity.

For rhombic truncated dodecahedral/icosahedral tensegrities, P_α ($\alpha = 1, 2, 3$) are

$$P_1 = -38880(Q_1 + Q_2)^5(Q_2^2 + 2Q_1Q_2 - Q_1 - Q_2)^4(5Q_2^2$$
$$+ 6Q_1Q_2 - 3Q_1 - 3Q_2)^4 \times (18Q_1^3Q_2 + 10Q_1Q_2^3$$
$$+ 30Q_1^2Q_2^2 - 9Q_1^3 - 5Q_2^3 - 33Q_1^2Q_2 - 29Q_1Q_2^2 + 6Q_1^2$$
$$+ 6Q_2^2 + 12Q_1Q_2)^5 \times [6(5 - \sqrt{5})Q_1^2Q_2 + 20Q_1Q_2^2 - 3(5$$
$$- \sqrt{5})Q_1^2 - 10Q_2^2 - 8(5 - \sqrt{5})Q_1Q_2 + 2(5 - \sqrt{5})Q_1$$
$$+ 2(5 - \sqrt{5})Q_2]^3 \times [6(5 + \sqrt{5})Q_1^2Q_2 + 20Q_1Q_2^2 - 3(5$$
$$+ \sqrt{5})Q_1^2 - 10Q_2^2 - 8(5 + \sqrt{5})Q_1Q_2 + 2(5 + \sqrt{5})Q_1$$
$$+ 2(5 + \sqrt{5})Q_2]^3, \quad (A.7)$$

$$P_2 = 25920P_{2,12}(Q_1 + Q_2)^4(Q_2^2 + 2Q_1Q_2 - Q_1 - Q_2)^3(5Q_2^2$$
$$+ 6Q_1Q_2 - 3Q_1 - 3Q_2)^3 \times (18Q_1^3Q_2 + 10Q_1Q_2^3$$
$$+ 30Q_1^2Q_2^2 - 9Q_1^3 - 5Q_2^3 - 33Q_1^2Q_2 - 29Q_1Q_2^2 + 6Q_1^2$$
$$+ 6Q_2^2 + 12Q_1Q_2)^4 \times [6(5 - \sqrt{5})Q_1^2Q_2 + 20Q_1Q_2^2 - 3(5$$
$$- \sqrt{5})Q_1^2 - 10Q_2^2 - 8(5 - \sqrt{5})Q_1Q_2 + 2(5 - \sqrt{5})Q_1$$
$$+ 2(5 - \sqrt{5})Q_2]^2 \times [6(5 + \sqrt{5})Q_1^2Q_2 + 20Q_1Q_2^2 - 3(5$$
$$+ \sqrt{5})Q_1^2 - 10Q_2^2 - 8(5 + \sqrt{5})Q_1Q_2 + 2(5 + \sqrt{5})Q_1$$
$$+ 2(5 + \sqrt{5})Q_2]^2, \quad (A.8)$$

$$P_3 = -17280P_{3,12}(Q_1 + Q_2)^3(Q_2^2 + 2Q_1Q_2 - Q_1 - Q_2)^2(5Q_2^2$$
$$+ 6Q_1Q_2 - 3Q_1 - 3Q_2)^2 \times (18Q_1^3Q_2 + 10Q_1Q_2^3$$
$$+ 30Q_1^2Q_2^2 - 9Q_1^3 - 5Q_2^3 - 33Q_1^2Q_2 - 29Q_1Q_2^2 + 6Q_1^2$$
$$+ 6Q_2^2 + 12Q_1Q_2)^3 \times [6(5 - \sqrt{5})Q_1^2Q_2 + 20Q_1Q_2^2 - 3(5$$
$$- \sqrt{5})Q_1^2 - 10Q_2^2 - 8(5 - \sqrt{5})Q_1Q_2 + 2(5 - \sqrt{5})Q_1$$
$$+ 2(5 - \sqrt{5})Q_2] \times [6(5 + \sqrt{5})Q_1^2Q_2 + 20Q_1Q_2^2 - 3(5$$
$$+ \sqrt{5})Q_1^2 - 10Q_2^2 - 8(5 + \sqrt{5})Q_1Q_2 + 2(5 + \sqrt{5})Q_1$$
$$+ 2(5 + \sqrt{5})Q_2], \quad (A.9)$$

where the specific expressions of $P_{2,12}$ and $P_{3,12}$ are omitted. Here the second index 12 stands for a rhombic truncated dodecahedral/icosahedral tensegrity.

References

Ali, N.B.H., Smith, I.F.C., 2010. Dynamic behavior and vibration control of a tensegrity structure. Int. J. Solids Struct. 47, 1285–1296.

Connelly, R., 1999. Tensegrity structures: why are they stable? In: Thorpe, M.F., Duxbury, P.M. (Eds.), Rigidity Theory and Applications. Kluwer Academic/Plenum Publishers, New York, pp. 47–54.

Connelly, R., Back, A., 1998. Mathematics and tensegrity. Am. Scientist 86, 142–151.

Coxeter, H.S.M., 1973. Regular Polytopes. Dover Publications, Inc., New York.

Cromwell, P.R., 1997. Polyhedra. Cambridge University Press, London.

Estrada, G.G., Bungartz, H.J., Mohrdieck, C., 2006. Numerical form-finding of tensegrity structures. Int. J. Solids Struct. 43, 6855–6868.

Feng, X.Q., Li, Y., Cao, Y.P., Yu, S.W., Gu, Y.T., 2010. Design methods of rhombic tensegrity structures. Acta Mech. Sin. 26, 559–565.

Fraternali, F., Senatore, L., Daraio, C., 2012. Solitary waves on tensegrity lattices. J. Mech. Phys. Solids 60, 1137–1144.

Guest, S.D., 2011. The stiffness of tensegrity structures. IMA J. Appl. Math. 76, 57–66.

Holst, J., Watson, S., Lord, M.S., Eamegdool, S.S., Bax, D.V., Nivison-Smith, L.B., Kondyurin, A., Ma, L.A., Oberhauser, A.F., Weiss, A.S., Rasko, J.E.J., 2010. Substrate elasticity provides mechanical signals for the expansion of hemopoietic stem and progenitor cells. Nat. Biotechnol. 28, 1123–1128.

Ingber, D.E., 2010. From cellular mechanotransduction to biologically inspired engineering. Ann. Biomed. Eng. 38, 1148–1161.

Juan, S.H., Tur, J.M.M., 2008. Tensegrity frameworks: static analysis review. Mech. Mach. Theory 43, 859–881.

Koohestani, K., 2012. Form-finding of tensegrity structures via genetic algorithm. Int. J. Solids Struct. 49, 739–747.

Lazopoulos, K.A., 2005. Stability of an elastic cytoskeletal tensegrity model. Int. J. Solids Struct. 42, 3459–3469.

Li, Y., Feng, X.Q., Cao, Y.P., Gao, H.J., 2010a. Constructing tensegrity structures from one-bar elementary cells. Proc. R. Soc. A 466, 45–61.

Li, Y., Feng, X.Q., Cao, Y.P., Gao, H.J., 2010b. A Monte Carlo form-finding method for large scale regular and irregular tensegrity structures. Int. J. Solids Struct. 47, 1888–1898.

Luo, Y.Z., Xu, X., Lele, T., Kumar, S., Ingber, D.E., 2008. A multi-modular tensegrity model of an actin stress fiber. J. Biomech. 41, 2379–2387.

Maina, J.N., 2007. Spectacularly robust! Tensegrity principle explains the mechanical strength of the avian lung. Respir. Physiol. Neuro. 155, 1–10.

Moored, K.W., Kemp, T.H., Houle, N.E., Bart-Smith, H., 2011. Analytical predictions, optimization, and design of a tensegrity-based artificial pectoral fin. Int. J. Solids Struct. 48, 3142–3159.

Morrison, G., Hyeon, C., Hinczewski, M., Thirumalai, D., 2011. Compaction and tensile forces determine the accuracy of folding landscape parameters from single molecule pulling experiments. Phys. Rev. Lett. 106, 138102.

Motro, R., 2003. Tensegrity: Structural Systems for the Future. Butterworth-Heinemann, London.

Murakami, H., Nishimura, Y., 2001. Static and dynamic characterization of regular truncated icosahedral and dodecahedral tensegrity modules. Int. J. Solids Struct. 38, 9359–9381.

Murakami, H., Nishimura, Y. 2003. Infinitesimal mechanism modes of tensegrity modules, in: Watanabe, K., Ziegler, F. (Eds.), Iutam Symposium on Dynamics of Advanced Materials and Smart Structures. Springer, Dordrecht, pp. 273–284.

Pagitz, M., Tur, J.M.M., 2009. Finite element based form-finding algorithm for tensegrity structures. Int. J. Solids Struct. 46, 3235–3240.

Pandia Raj, R., Guest, S.D., 2006. Using symmetry for tensegrity form-finding. J. Int. Assoc. Shell Spatial Struct. 47, 245–252.

Pirentis, A.P., Lazopoulos, K.A., 2010. On the singularities of a constrained (incompressible-like) tensegrity–cytoskeleton model under equitriaxial loading. Int. J. Solids Struct. 47, 759–767.

Pugh, A., 1976. An Introduction to Tensegrity. University of California Press, Berkely.

Rhode-Barbarigos, L., Ali, N.B.H., Motro, R., Smith, I.F.C., 2010. Designing tensegrity modules for pedestrian bridges. Eng. Struct. 32, 1158–1167.

Schek, H.J., 1974. The force density method for form finding and computation of general networks. Comput. Meth. Appl. Mech. Eng. 3, 115–134.

Schenk, M., Guest, S.D., Herder, J.L., 2007. Zero stiffness tensegrity structures. Int. J. Solids Struct. 44, 6569–6583.

Skelton, R.E., de Oliveira, M.C., 2009. Tensegrity Systems. Springer, Dordrecht.

Stamenovic, D., Ingber, D.E., 2009. Tensegrity-guided self assembly: from molecules to living cells. Soft Matter 5, 1137–1145.

Sultan, C., 2009. Tensegrity: 60 years of art, science, and engineering. In: Aref, H., van der Giessen, E. (Eds.), Advances in Applied Mechanics. Elsevier Academic Press Inc., San Diego, pp. 69–145.

Tibert, A.G., Pellegrino, S., 2003. Review of form-finding methods for tensegrity structures. Int. J. Space Struct. 18, 209–223.

Tran, H.C., Lee, J., 2010. Advanced form-finding for cable-strut structures. Int. J. Solids Struct. 47, 1785–1794.

Vassart, N., Motro, R., 1999. Multiparametered formfinding method: application to tensegrity systems. Int. J. Space Struct. 14, 147–154.

Xu, X.A., Luo, Y.Z., 2011. Multistable tensegrity structures. J. Struct. Eng. ASCE 137, 117–123.

Yuan, X., Chen, L., Dong, S., 2007. Prestress design of cable domes with new forms. Int. J. Solids Struct. 44, 2773–2782.

Zhang, J.Y., Ohsaki, M., 2006. Adaptive force density method for form-finding problem of tensegrity structures. Int. J. Solids Struct. 43, 5658–5673.

Zhang, J.Y., Ohsaki, M., 2007. Stability conditions for tensegrity structures. Int. J. Solids Struct. 44, 3875–3886.

Zhang, J.Y., Ohsaki, M., 2012. Self-equilibrium and stability of regular truncated tetrahedral tensegrity structures. J. Mech. Phys. Solids 60, 1757–1770.

Zhang, L.Y., Li, Y., Cao, Y.P., Feng, X.Q., Gao, H.J., 2012. Self-equilibrium and super-stability of truncated regular polyhedral tensegrity structures: a unified analytical solution. Proc. R. Soc. A 468, 3323–3347.